ResearchGate

See discussions, stats, and author profiles for this publication at: https://www.researchgate.net/publication/262304423

A Robust Pathway to Electrically Conductive Hemicellulose Hydrogels with High and Controllable Swelling Behavior

ARTICLE *in* POLYMER · JUNE 2014

Impact Factor: 3.56 · DOI: 10.1016/j.polymer.2014.05.003

CITATIONS
10

READS
58

5 AUTHORS, INCLUDING:

Weifeng Zhao
Sichuan University
34 PUBLICATIONS **569** CITATIONS
SEE PROFILE

Karin Odelius
KTH Royal Institute of Technology
37 PUBLICATIONS **483** CITATIONS
SEE PROFILE

Ulrica Edlund
KTH Royal Institute of Technology
74 PUBLICATIONS **1,780** CITATIONS
SEE PROFILE

Ann-Christine Albertsson
KTH Royal Institute of Technology
419 PUBLICATIONS **11,374** CITATIONS
SEE PROFILE

All in-text references underlined in blue are linked to publications on ResearchGate, letting you access and read them immediately.

Available from: Weifeng Zhao
Retrieved on: 24 January 2016

Polymer 55 (2014) 2967–2976

Contents lists available at ScienceDirect

Polymer

journal homepage: www.elsevier.com/locate/polymer

A robust pathway to electrically conductive hemicellulose hydrogels with high and controllable swelling behavior

Weifeng Zhao [a,b], Lidija Glavas [a], Karin Odelius [a], Ulrica Edlund [a], Ann-Christine Albertsson [a,*]

[a] Fiber and Polymer Technology, School of Chemical Science and Engineering, Royal Institute of Technology (KTH), Teknikringen 56-58, SE-100 44 Stockholm, Sweden
[b] College of Polymer Science and Engineering, State Key Laboratory of Polymer Materials Engineering, Sichuan University, Chengdu 610065, Sichuan, China

ARTICLE INFO

Article history:
Received 11 February 2014
Received in revised form
8 April 2014
Accepted 2 May 2014
Available online 14 May 2014

Keywords:
Hydrogels
Hemicellulose
Electrically conductive

ABSTRACT

A robust pathway to synthesize electrically conductive hemicellulose hydrogels (ECHHs) based on *O*-acetyl-galactoglucomannan (AcGGM) and conductive aniline tetramer (AT) is presented. These ECHHs were obtained by functionalizing carboxylated AcGGM with glycidyl methacrylate (GMA) and subsequently covalently immobilizing AT onto GMA. Hydrogel swelling ratios (SRs) were regulated by the degree of substitution (DS) of the carboxylated AcGGM, the maximum varied as follows: $SR_{DS=1.14} < SR_{DS=0.60} < SR_{DS=0.24}$. The SR can also be tuned from 548% to 228% by changing the AT contents from 10% (w/w) to 40% (w/w) while simultaneously altering conductivities from 2.93×10^{-8} to 1.12×10^{-6} S/cm. Free-standing ECHHs with tunable conductivity and degree of swelling, as presented herein, have a broad potential for biomedical applications.

© 2014 The Authors. Published by Elsevier Ltd. This is an open access article under the CC BY-NC-ND license (http://creativecommons.org/licenses/by-nc-nd/3.0/).

1. Introduction

Polymeric hydrogels have defined a remarkable research area, mainly due to their wide range of applications, such as matrix chemistry and biology [1], the removal of endocrine disruptors [2], media for the delivery of substances in biomedicine [3], and scaffolds [4]. Hydrogels have potential in biomedical applications due to their good biocompatibility and ability to selectively mimic human tissues [1,5]. Natural polymer-based hydrogels, such as those made from proteins and polysaccharides, are widely used in injectable engineering [6], controlled drug release [7,8], biosensors [9], and articular cartilage tissue engineering [10] because they are commonly biocompatible, degradable, capable of promoting cell adhesion and proliferation, and immunologically inert. Hemicellulose-based hydrogels are currently being acknowledged for their non-toxic and renewable properties in addition to the advantages of natural polymers mentioned above [11–15].

The family of hemicelluloses is the second most abundant group of polysaccharides in the vegetal world after cellulose, representing 15–35% (w/w) of higher plants and wood [16]. The pendant hydroxyl groups of the polysaccharide backbone offer a number of possibilities for the chemical modification of hemicelluloses and for the preparation of materials with new profiles that can increase the utility of these biopolymers. The preparation of biomedical hemicellulose materials, such as bio-sorbents and hydrogels, may be useful in key applications, such as heavy metal removal [17], drug release systems, and tissue engineering [18,19]. For gymnosperms, glucomannan is the major type of hemicellulose in the secondary cell wall, where it is also believed to serve a structural function [20]. Due to the abundance, the relatively high degree of acetylation and the low molecular weight of *O*-acetyl-galactoglucomannan (AcGGM), in addition to its solubility in water and in dimethyl sulfoxide (DMSO) and dimethylformamide (DMF), it serves as an attractive renewable material candidate for the design of hydrogels [13,19]. AcGGM-derived hydrogels have recently been prepared by a carbonyldiimidazole (CDI)-assisted coupling reaction between AcGGM and hydroxyethyl methacrylate (HEMA) followed by cross-linking of the vinyl functional groups. Microspheres prepared from AcGGM-based hydrogels and loaded with either a small hydrophilic substance (caffeine) or a macromolecular model protein (bovine serum albumin) showed controlled release *in vitro* [14]. Furthermore, it was demonstrated that both the pendant group composition and the enzyme action are valuable tools in the tailoring of hydrogel release profiles for drug delivery [19]. A series of cross-linking chemistries for AcGGM-based hydrogels was also developed, and the resulting properties of the AcGGM gels could be

* Corresponding author. Tel.: +46 8 790 8274; fax: +46 8 208 477.
E-mail addresses: aila@kth.se, aila@polymer.kth.se (A.-C. Albertsson).

http://dx.doi.org/10.1016/j.polymer.2014.05.003
0032-3861/© 2014 The Authors. Published by Elsevier Ltd. This is an open access article under the CC BY-NC-ND license (http://creativecommons.org/licenses/by-nc-nd/3.0/).

custom-built for a specific performance [13,21]. However, electrical conductivity is rarely investigated in hemicellulose-derived materials, although conductivity features could promote polymer–cell interactions that would be useful in a wide range of applications in the biomedical field. For instance, conductive properties have been shown to support the attachment and differentiation of neural-like cells with improved interactions [22], and biomaterials with electrical conductivity have the potential to be used in nerve regeneration [23].

The term *conductive polymers* (CPs) denotes organic polymers that exhibit similar properties to those of metals and inorganic semiconductors and are considered as the fourth generation of polymeric materials [23,24]. The explosive growth of research on CPs is due to their interesting physical and chemical properties, such as electrical conductivity, electroluminescence, and electrochromism, which are useful in a number of practical applications, e.g., photovoltaic devices, light-emitting diodes, electrochromic displays and biomedical devices [23,25]. Polyaniline (PANi) and its derivatives are the most commonly investigated CPs in biomedical engineering. For example, porous tubular scaffolds fabricated from blends of polycaprolactone (PCL) and a hyperbranched conducting copolymer show non-cytotoxicity with HaCaT keratinocytes [26]. Guarino et al. demonstrated that conductive PANi/PEGDA macroporous hydrogels improve the biological response of PC12 and hMSC cells [23]. One drawback associated with these conductive composites is that the scaffold-forming components (e.g., PCL and PEGDA) are non-renewable materials. In addition, PANi has poor solubility in most solvents [27]. One approach to overcoming this predicament is to design aniline oligomers with biodegradable and renewable resources [25]. Chen et al. developed new biodegradable electroactive hydrogels with aniline pentamer grafted onto gelatin [28], and aniline pentamer for cross-linking chitosan [29]. The preliminary study demonstrated that these hydrogels have the potential to be utilized in drug delivery and tissue engineering. We anticipate that electrically conductive hemicellulose hydrogels (ECHHs) could be obtained by combining a conductive aniline tetramer with biodegradable and nontoxic hemicellulose. Therefore, ECHHs provide a potential means to electrically simulate cells and regulate specific cellular activities to widely extend the applications of CPs in biomedical fields, such as controlled drug release and nerve regeneration.

Our aim is to develop a robust synthetic route for ECHHs by covalently attaching conductive aniline tetramers to AcGGM-derived hydrogels. The introduction of maleic anhydride, glycidyl methacrylate and conductive aniline tetramer into the polysaccharide scaffold will alter the swelling ratio and enable control over the hydrogel properties. Our aim is further to regulate the conductivity by altering the aniline tetramer content.

2. Experimental section

2.1. Materials

Glycidyl methacrylate (GMA), triethylamine (TEA), maleic anhydride (MA), N-phenyl-p-phenylenediamine, ammonium persulfate (APS), ammonium hydroxide (NH_4OH), hydrochloric acid (HCl), dimethyl sulfoxide (DMSO), N,N-dimethylacetamide (DMAc) and tetrahydrofuran (THF) were purchased from Sigma–Aldrich and were used as received, unless otherwise stated. *O*-acetyl-galactoglucomannan (AcGGM) originating from spruce (*Picea abies*) was extracted from thermo-mechanical pulping (TMP) processed water, purified and concentrated by ultrafiltration (membrane cutoff 1 kDa), and lyophilized using a Lyolab 300 lyophilizer. The carbohydrate composition of the AcGGM isolate was 17 mol% glucose, 65 mol% mannose, and 15 mol% galactose. AcGGM had a number average molecular weight (M_n) of approximately 7500 g mol^{-1} (DP ~ 40), a dispersity index ($Đ$) of 1.3 and a degree of acetylation (DS_{Ac}) of 30%, as determined by size exclusion chromatography (SEC) calibrated with MALDI-TOF according to a published protocol [30].

2.2. Synthesis of aniline tetramer

Aniline tetramer (AT) was synthesized according to a previously described procedure [31]. Briefly, N-phenyl-p-phenylenediamine (3.68 g, 0.02 mol) was dissolved in a 150 mL mixture of acetone with 1 mol/L HCl (v/v 150:100) at 0 °C. Ammonium persulfate (9.12 g, 0.04 mol) in 100 mL of acetone/HCl solution was then added dropwise to the solution over 30 min. A color change from green to dark blue was observed, and the reaction was allowed to proceed for another 2 h at 0 °C. The mixture was subsequently filtered, and the filter cake was washed with 1 M HCl and deionized water. The crude AT was dedoped in 1 M NH_4OH for 2 h and then filtered and washed with deionized water until the filtrate was neutral. Finally, the AT (dark powder, yield 68.5%) was lyophilized for 3 days.

2.3. Synthesis of carboxylated AcGGM (C-AcGGM)

C-AcGGM was prepared as previously reported [32] with some small modifications (Scheme 1). In brief, 1 g of AcGGM (~5.7 mmol sugar units) was dissolved in 30 mL of pre-dried DMSO at 50 °C. TEA (0.1 mL) and 0.14–0.58 g of MA (1.4–5.7 mmol, 0.25–1 eq) were added. The reaction mixture was kept at 50 °C for 1 h. The reaction was quenched by pouring the reaction mixture into 200 mL of THF, and the solid residue was collected by centrifugation. The product was washed with 300 mL of THF and dried under reduced pressure. To investigate the effect of the degree of

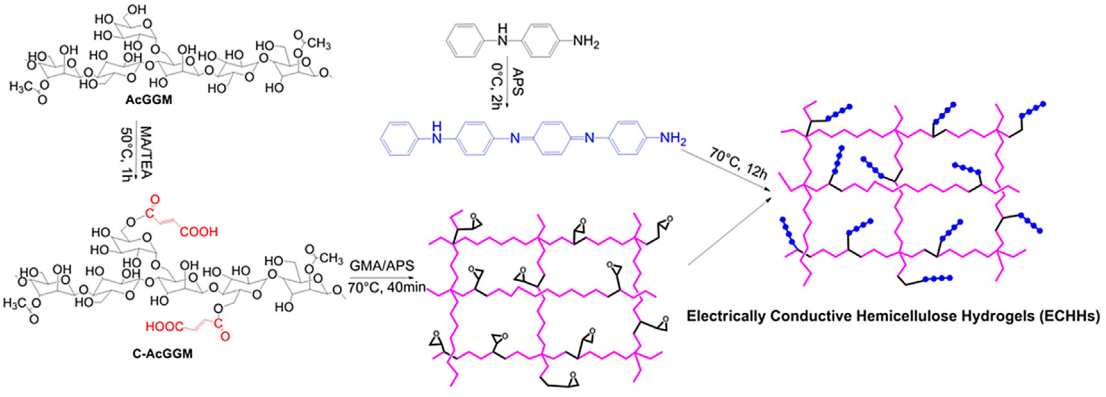

Scheme 1. Proposed synthesis route of electrically conductive hemicellulose hydrogels (ECHHs).

substitution of MA on the swelling ratio (SR) of the hemicellulose hydrogels, the precursor C-AcGGM polymers were prepared with 0.25, 0.5 and 1.0 eq of MA and denoted as C0.25-AcGGM, C0.5-AcGGM and C1.0-AcGGM, respectively. The degree of substitution (DS) was determined by ^{1}H NMR spectroscopy. Yield: 90–99%.

2.4. Preparation of ECHHs

ECHHs were prepared by a two-step reaction (Scheme 1) with varying feed compositions (Table 1). In brief, 200 mg of C1.0-AcGGM was dissolved in 0.8 mL of DMSO followed by the addition of 60 mg of APS and 100 mg of GMA. The mixture was degassed prior to the reaction. The cross-linking reaction was conducted at 70 °C for 40 min. Subsequently, the formed gel was purified in DMSO to remove the unreacted residues. The gel was immersed in a DMSO solution with different concentrations of AT and kept at 70 °C for 12 h followed by washing in DMSO for 48 h. DMSO was changed frequently (every 2 h in the beginning) to ensure complete removal of unreacted AT. Then, a H_2O/THF mixture (v/v 1:1) was used to remove DMSO. Finally, the ECHHs were dried under vacuum for 3 days.

The ECHHs with 10, 20, 30 and 40% (w/w) AT were annotated according to their equivalent of MA, the addition of GMA and the % (w/w) of AT. As an example, C1.0-AcGGM/GMA/10%AT contained 200 mg of C1.0-AcGGM, 100 mg of GMA and 10% (w/w) AT. A gel without AT was synthesized as a reference sample and denoted C1.0-AcGGM/GMA. The gels prepared from C0.25-AcGGM, C0.5-AcGGM and C1.0-AcGGM polymers were used to investigate the effect of the degree of substitution of MA on the swelling ratio (SR) of the hemicellulose hydrogels.

2.5. Characterization

^{1}H NMR (400 MHz) spectra of AT, AcGGM and C-AcGGM polymers and ^{13}C NMR (400 MHz) spectra of AcGGM and C-AcGGM polymers were obtained using a Bruker Avance 400 MHz NMR instrument at room temperature with DMSO-d_6 as the solvent and the residual DMSO as the internal standard ($\delta = 2.50$).

Matrix-assisted laser desorption/ionization time of flight (MALDI-TOF) was used to verify the successful synthesis of AT. MALDI-TOF analyses were performed on a Bruker Ultraflex MALDI-TOF mass spectrometer with a SCOUT-MTP Ion Source (Bruker Daltonics, Bremen) equipped with a N_2 laser (337 nm), a grid-less ion source, and a reflector design. The positive ion spectra depicted are representations of the sums of 1000 laser shots. The instrument operated at an acceleration voltage of 25 kV and a reflector voltage of 26.3 kV, and the detector mass range was set to 60–1000 Da. Samples were prepared by dropping 1–3 μL of samples (1 mg/mL DMSO solution) onto a steel coordinate plate. MALDI data were collected and analyzed with FlexAnalysis software (Bruker Daltonics).

Table 1
Feed compositions of ECHHs.

Sample codes	mol% of MA	C-AcGGM (mg)	GMA (mg)	DMSO (mL)	AT[a] (mg)
C1.0-AcGGM	100	200		0.8	
C0.5-AcGGM	50	200		0.8	
C0.25-AcGGM	25	200		0.8	
C1.0-AcGGM/GMA	100	200	100	0.8	
C1.0-AcGGM/GMA/10%AT	100	200	100	0.8	33
C1.0-AcGGM/GMA/20%AT	100	200	100	0.8	75
C1.0-AcGGM/GMA/30%AT	100	200	100	0.8	130
C1.0-AcGGM/GMA/40%AT	100	200	100	0.8	200

[a] The amount of AT in 4 mL of DMSO.

FTIR spectra were recorded using a Perkin Elmer Spectrum 2000 spectrometer (Perkin–Elmer Instrument, Inc.) equipped with a single reflection attenuated total reflectance (ATR) accessory (golden gate) from Graseby Specac (Kent, UK). FTIR was used to verify the molecular structures of AT, the AcGGM and C-AcGGM polymers. FTIR was also utilized to verify the successful coupling of AT to the hemicellulose hydrogels. Each spectrum was recorded as the average of 16 scans at a resolution of 4 cm^{-1} in the range between 4000 and 600 cm^{-1}.

The water contact angle measurements of C1.0-AcGGM, C1.0-AcGGM/GMA and C1.0-AcGGM/GMA/10%AT hydrogels films were measured using a contact angle and surface tension meter (KSV instruments Ltd.). A drop of Milli-Q water (5 μL) was placed on the surface of the sample and images of the water menisci were recorded by a digital camera. The contact angle of each sample was taken as the average of four measurements at different points.

Size exclusion chromatography (SEC) was used to determine the molecular weight and dispersity index ($Đ$) of AcGGM and C-AcGGM [33]. The samples were analyzed using a Shimidzu RID-10A SEC equipped with a refractive index detector and three PLgel 20 μm Mixed-A (300 mm × 7.5 mm) columns with an injection volume of 200 μL. Dimethylacetamide (DMAc) with 0.05% (w/w) LiCl was used as the eluent (0.5 mL/min). The measurements were performed at 80 °C. The SEC system was calibrated with Pullulan standards with molecular weights ranging from 342 to 800,000 g/mol. The samples were dissolved in DMAc (0.05% (w/w) LiCl) by vigorous stirring and filtered (0.45 μm, Millipore) before injection. LC Solution software from Shimatzu was used for data acquisition and calculations.

The swelling ratio (SR) of the hydrogels was determined by immersing pre-weighed dry hydrogels in buffer solutions (prepared from Na_2HPO_4 and NaH_2PO_4, pH = 7.4) at room temperature. The weight gain of the hydrogels was monitored gravimetrically as a function of time. The weights of the samples in the swollen state at different times t (m_t) were measured after gently removing excess water using filter paper. The SR was calculated using Eq. (1), where m_0 denotes the weight of the samples in the dry state:

$$\mathrm{SR}(\%) = \frac{m_t - m_0}{m_0} \times 100 \quad (1)$$

For the thermal stability of the hydrogels, thermogravimetric analysis (TGA) of the samples was performed using a Mettler-Toledo TGA/SDTA 851e. Approximately 10 mg of each sample was put into a 70 μL ceramic cup without a lid. TGA tests were conducted under a nitrogen atmosphere (flow rate of 50 mL/min) with a heating rate of 10 °C/min from 30 to 800 °C. The data were collected and analyzed by Mettler STARe software.

The cross-section morphology of the hydrogels was observed by Ultra-High Resolution FE-SEM (Hitachi S-4800). The samples were lyophilized overnight in small vials, cross-sectioned, attached to the sample supports and coated with a 3 nm gold layer.

The electrical conductivity of the 1 mol/L HCl-doped hydrogels was determined by the standard Van der Pauw four-probe method (two reference probes, one counter probe and one working probe) [31,34]. After doping, the hydrogels were thoroughly dried in a vacuum oven for 48 h. Therefore, the conductivity of the hydrogel was not affected by water content. Hydrogel pellets, with a diameter of 2 cm and a thickness ranging from 0.035 to 0.050 cm, were made by compression molding using a pressure of 30 kN/m^2 at 70 °C for 10 min.

3. Results and discussion

Hemicellulose-based hydrogels are being developed due to their biocompatibility, nontoxicity and abundantly renewability [14,23].

Aniline oligomers exhibit similar conductivity with improved process-ability compared to metals and inorganic semiconductors [27]. Therefore, a new family of electrically conductive hemicellulose hydrogels (ECHHs) was developed in this work by combining *O*-acetyl-galactoglucomannan (AcGGM) and aniline tetramer (AT). AcGGM was carboxylated with varying amounts of MA (C-AcGGM) to regulate the swelling behavior of hydrogels. The reaction pathway was tuned to be robust so that it can be carried out under ambient conditions without requiring inert atmospheres or dry conditions. Varying amounts of AT were immobilized into the hydrogels to provide conductivity and further regulate the swelling behavior of hydrogels.

3.1. Synthesis of AT

The successful synthesis of AT was verified by NMR and MALDI-TOF mass spectrometry. The ^{1}H NMR spectrum of AT is shown in the Supporting Information (Fig. S1). There is a single peak at 5.53 ppm and no peak at 4.69 ppm, indicating that only one isomer exists in the DMSO solution [35]. AT appeared as a peak at 366.36 *m*/*z* in MALDI-TOF mass spectra, which matched its chemical structure. These results agree with previous reports [31,35].

3.2. Synthesis of C-AcGGM polymers

To achieve a facile and robust gelation, the heteropolysaccharide AcGGM was modified with MA under ambient conditions to covalently immobilize double bonds for subsequent *in situ* gelation. A series of C-AcGGM with varying degrees of substitution of MA were prepared to tune the swelling behavior.

ATR-FTIR spectra confirmed the structural composition of pure AcGGM and C-AcGGM polymers (Fig. 1). Pristine AcGGM displayed the anticipated C=O stretching at 1730 cm^{-1} stemming from the acetylated pendant groups, a H–O–H deformation vibration of absorbed water at approximately 1643 cm^{-1}, some alkane vibrations in the 1350–1480 cm^{-1} region, and a hydroxyl band at 3000–3600 cm^{-1} (Fig. 1A). In contrast, AcGGM modified with MA (C-AcGGM) displayed an increase in band intensity at 1721 cm^{-1}, attributed to the C=O functionality of the ester linkage. The peaks emerging at 1638, 1581 cm^{-1} and 950 cm^{-1} were due to the C=C stretching and deformation vibrations, verifying the presence of vinyl groups in the modified AcGGM. The peak emerging at 1165 cm^{-1} was attributed to the vibration of the methylene group in each substituted C-6 position. All results agree with our previous reports [13,32]. The intensity of the peaks at 1721 and 1581 cm^{-1} increased with an increase in the MA content (Fig. 1B), indicating the successful coupling of MA to AcGGM. The intensity of the peaks in the 966–1133 cm^{-1} region (–C–O–C– vibrations from the sugar units) should remain constant since there was almost no change for –C–O–C– bonds during the reaction. Therefore, the ratio (*R*) of the area of the peaks in the 1674–1776 cm^{-1} region ($A_{1674-1776}$) to the area of the peaks in the 966–1133 cm^{-1} region ($A_{966-1133}$) reflects the grafting density (GD) of MA, which is defined in Eq. (2). The GD increased with the increase of the mole ratio of MA, as shown in Supporting Information (Table S1).

$$\mathrm{GD}(\%) = \frac{R_{\mathrm{C-AcGGM}} - R_{\mathrm{AcGGM}}}{R_{\mathrm{AcGGM}}} \times 100 \qquad (2)$$

^{1}H and ^{13}C NMR were further used to confirm the successful coupling of AcGGM with MA and to determine the degree of substitution (DS) achieved in the reaction (Fig. 2 and Fig. S2). Upon coupling, additional peaks originating from the double bonds of MA appeared at 6.07 and 6.41 ppm, and a peak corresponding to the protons from the C-6 position of carboxylated AcGGM appeared at 3.10 ppm. In the ^{13}C NMR, alkene signals were observed at 128.61 and 132.43 ppm, while the carbonyls originating from the ester and carboxyl groups were observed at 165.52 and 167.05 ppm, respectively. As expected, a clear relationship between the DS and the amount of MA was found. As the degree of acetylation for the AcGGM used was determined to be 0.3 [30], the DS (the degree of carboxyl group substitution) can be calculated by setting the relative integral of the response of the alkene protons (6.41 and 6.07 ppm) in relation to the integral of the response of the acetyl protons (2.0 ppm). The DS increased with increased feed ratios of MA (Table 2).

3.3. Preparation of ECHHs

AT is a free radical inhibitor [36]; therefore, using free radical chemistry to incorporate AT into polymers is not a viable option

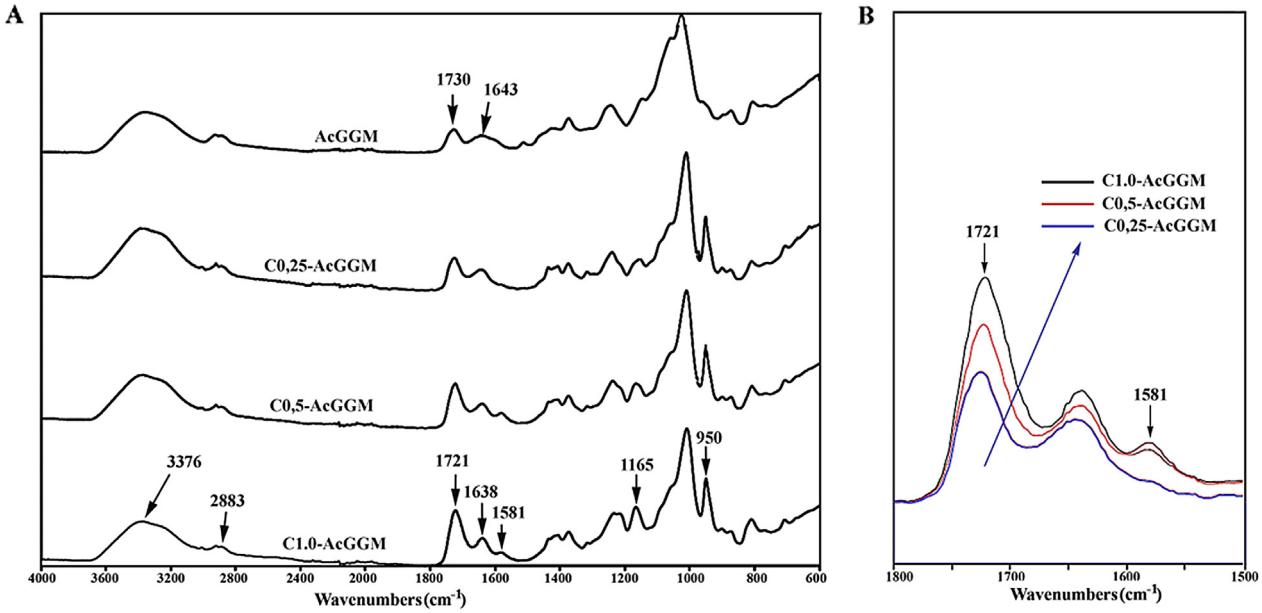

Fig. 1. ATR-FTIR spectra of pure and carboxylated AcGGM: split spectra (A) and overlay spectra (B) of C-AcGGM normalized at 1816 cm^{-1}.

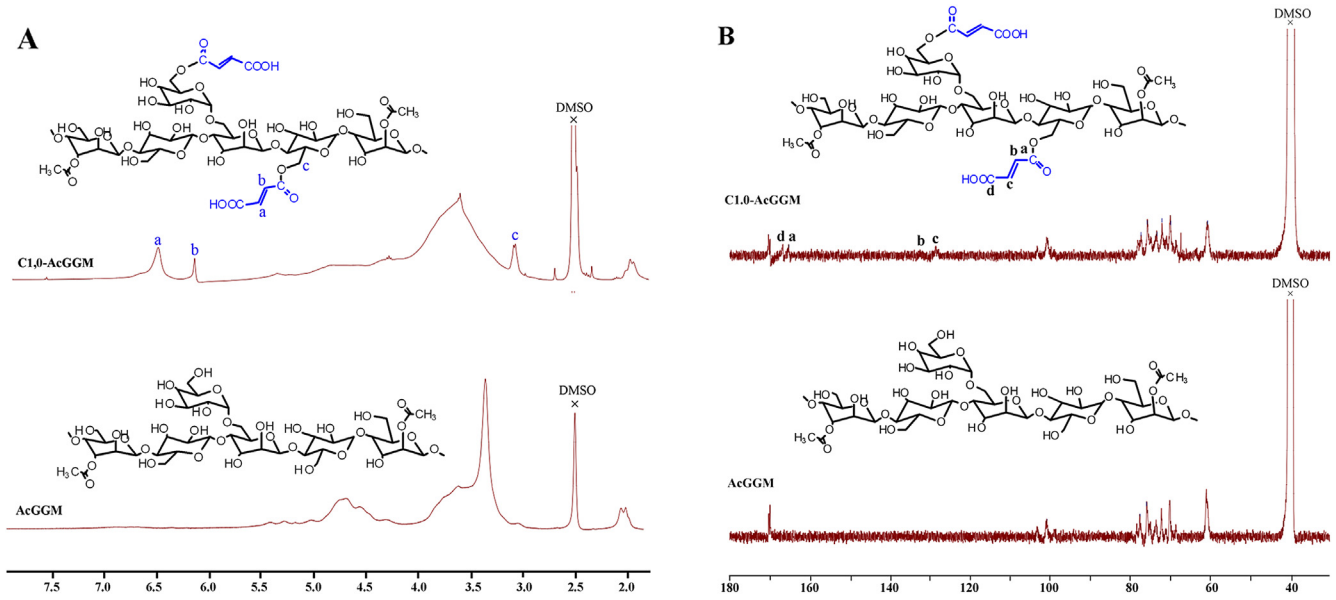

Fig. 2. ^{1}H NMR (A) and ^{13}C NMR (B) spectra of pristine AcGGM and C-AcGGM in DMSO-d_6.

unless the NH-groups in AT are protected [37]. There is also a need to deprotect the tert-butoxycarbonyl group in the polymer by heating or by acidic hydrolysis, methods that may cause an onset of the degradation of polysaccharides. To address this, we developed an alternative route involving the introduction of GMA into the hydrogel network. This was followed by chemical coupling of the AT segments to the network to form ECHHs by reacting the amino group in AT and the epoxy group in GMA. The hydrogels were prepared in two steps: (1) using ammonium persulfate to initiate polymerization of a mixture of C1.0-AcGGM and GMA, and (2) immersing the formed hydrogels in a DMSO solution containing varying amounts of AT. Compared to the functionalization of polymers with aniline oligomers using N,N′-dicyclohexyl carbodiimide/4-dimethylaminopyridine (DCC/DMAP) [38] or 1-ethyl-3-(3-dimethylaminopropyl)carbodiimide (EDC)/DMAP [39], the pathway presented here is more robust as there is no need to run the reactions under an inert atmosphere or to perform tedious and chemical-consuming purification procedures.

Table 2
Yield, number average molecular weight (M_n), dispersity index ($Đ$) and degree of substitution (DS) of C-AcGGM polymers.

Sample codes	Feed ratio of MA (FR)	Yield (%)	[a] M_n (g/mol)	[b] M_n (g/mol)	[b] DS	[c] M_n (g/mol)	[c] $Đ$
AcGGM						4400	3.07
C0.25-AcGGM	0.25	99	8444	7927	0.24	5300	2.92
C0.5-AcGGM	0.5	90	8669	8364	0.60	6050	2.67
C1.0-AcGGM	1.0	99	11 575	10 249	1.14	6000	2.22

[a] Calculated from feed ratio, taking the yield into consideration, $M_n = 7500 \times (1 + 0.57 \times FR \times 98.06) \times$ Yield.
[b] Determined by ^{1}H NMR.
[c] Determined by DMAc-SEC.

The hydrogel color changed from yellow (in web version) to opaque after adding GMA and then to black after the reaction with AT due to the color of AT (Fig. 3). Interestingly, the volume of hydrogels decreased in each step as a consequence of the hydrophobic nature of GMA and AT. The hydrophilicity of the hydrogels was systematically investigated and is discussed in the next section. The formed ECHHs were free-standing, indicating sufficient mechanical integrity for soft tissue scaffold applications (Fig. 3D).

ATR-FTIR was used to follow the formation of these ECHHs. The ATR-FTIR spectra of AT, C1.0-AcGGM, C1.0-AcGGM hydrogel, C1.0-AcGGM/GMA hydrogel and C1.0-AcGGM/GMA/10%AT hydrogel are shown in Fig. 4. The disappearance of the peak at 950 cm^{-1} corresponding to the double bonds (C=C) in the C-AcGGM polymer correlated with the crosslinking via radical polymerization. A new peak at 903 cm^{-1} assigned to the epoxy group in GMA is evident in curve C. The epoxy peak significantly diminished in curve D, while new peaks at 1580 cm^{-1} and 1500 cm^{-1} corresponding to the benzene and quinoid rings in AT, appeared. All of these results demonstrated that the C-AcGGM/GMA/AT hydrogels were successfully synthesized.

To verify that AT was covalently attached throughout the bulk of the hydrogels, the composition of C1.0-AcGGM/10%AT was assessed

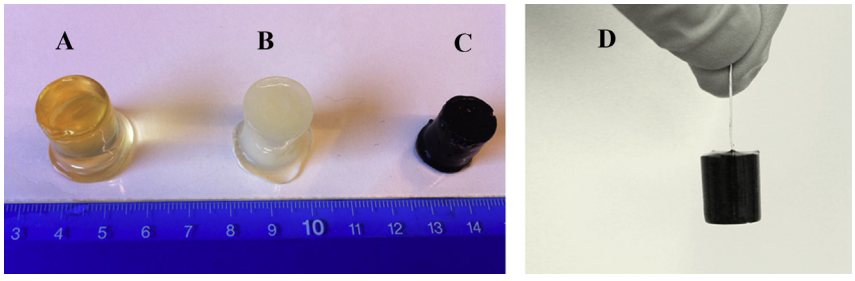

Fig. 3. Hydrogels based on C1.0-AcGGM (A), C1.0-AcGGM/GMA (B), and C1.0-AcGGM/GMA/10%AT (C), and free-standing C1.0-AcGGM/GMA/10%AT hydrogel (D).

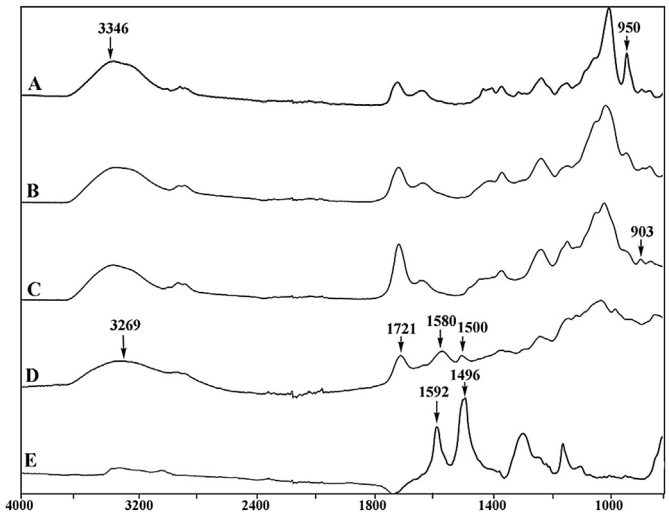

Fig. 4. ATR-FTIR spectra of C1.0-AcGGM (A), cross-linked C1.0-AcGGM hydrogel (B), C1.0-AcGGM/GMA hydrogel (C), C1.0-AcGGM/GMA/10%AT hydrogel (D), and AT (E).

at different positions. The ATR-FTIR spectra of the cross-section of C1.0-AcGGM/GMA/10%AT hydrogels indicated that the covalently attached AT-containing hydrogel, C1.0-AcGGM/GMA/10%AT, had equivalent AT intensities (characteristic peaks at approximately 1580 and 1500 cm^{-1}) from the surface to the center and is therefore homogeneously modified (Fig. 5).

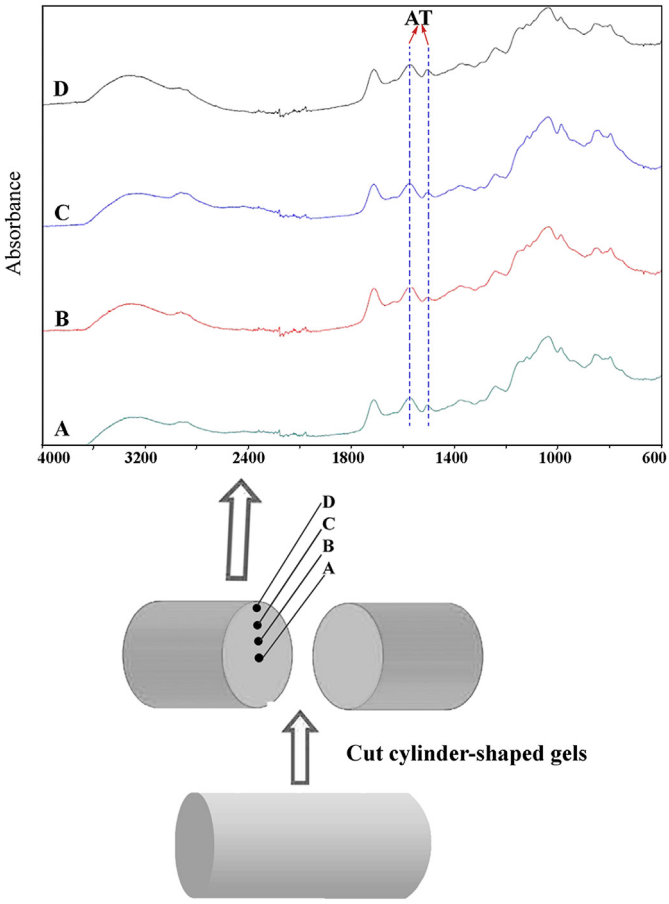

Fig. 5. ATR-FTIR spectra for the hydrogel with AT covalently attached, C1.0-AcGGM/GMA/10%AT, at different positions through the hydrogels.

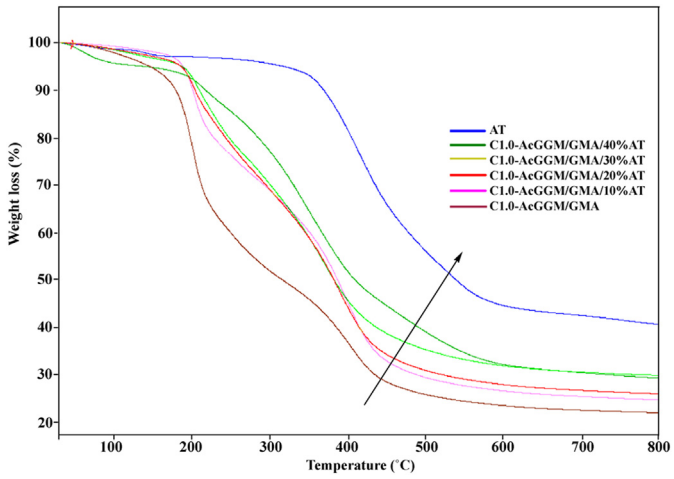

Fig. 6. TGA thermograms of AT and ECHHs.

3.4. Thermal properties of ECHHs

As the thermal properties of AcGGM and AT are different, their thermal behavior yields information about the composition of ECHHs. Therefore, thermogravimetric analysis (TGA) was utilized to characterize thermal behavior (Fig. 6). For the conductive hydrogels, the degradation was a two-step process. The largest weight losses for these hydrogels occurred between 210 °C and 400 °C and was dependent on the AT contents. This was attributed to the decomposition of AcGGM and GMA. The weight loss in the temperature range from 30 to 210 °C was due to desorption of incorporated water and other low molecular weight species [40]. Although all samples were freeze-dried in the same manner before the measurement, the water content was found to be between 2% and 10% for all hydrogels. The second mass loss occurred from 400 to 600 °C and is assigned to the degradation of the AT segments linked to the hydrogel network, after which the weight loss of the C1.0-AcGGM/GMA/AT hydrogels leveled off at temperature of approximately 600 °C. As expected, the thermal stability of the hydrogels increased with increasing AT content in the hydrogel, which is most likely due to the greater thermal stability of the AT segments [40,41]. According to the TGA curve, the weight loss percentages of the C1.0-AcGGM/GMA hydrogel and ECHHs in the range of 210–600 °C are W_R and W_H, respectively. The grafting amount of AT segments (W%) is defined by Eq. (3), where W_{AT} is the weight loss percentage of pure AT in the range of 210–600 °C, and W% represents the weight percentage of the AT segment connected to the hydrogel:

$$W\% = \frac{W_R - W_H}{W_H} \times 100 \quad (3)$$

The theoretical and measured grafting amounts of AT for each hydrogel are listed in Table 3. As anticipated, the AT contents calculated from TGA were slightly lower than the theoretical

Table 3
Conductivity and composition of ECHHs.

Sample codes	Conductivity (S/cm)	AT content from TGA (theoretical)
C1.0-AcGGM/GMA	$<10^{-10}$	–(0%)
C1.0-AcGGM/GMA/10%AT	$(2.93 \pm 0.32) \times 10^{-8}$	5.2% (10%)
C1.0-AcGGM/GMA/20%AT	$(8.49 \pm 0.45) \times 10^{-8}$	9.4% (20%)
C1.0-AcGGM/GMA/30%AT	$(1.30 \pm 0.21) \times 10^{-7}$	18.7% (30%)
C1.0-AcGGM/GMA/40%AT	$(1.12 \pm 0.14) \times 10^{-6}$	29.2% (40%)

calculations due to the incomplete reaction of AT with the epoxy groups in the hydrogel networks in the DMSO solution.

3.5. Conductivity of ECHHs

The electrical conductivities of the ECHHs with different contents of covalently attached AT were determined after doping with an equal amount of 1 mol/L HCl via a four-probe method. The conductivity of the hydrogel without AT was below the detector limit of the instrument ($<10^{-10}$ S/cm),which indicated the hydrogel without AT had extremely low or no conductivity. The conductivities of the hydrogels with AT contents from 10% (w/w) to 40% (w/w) range from $(2.93 \pm 0.32) \times 10^{-8}$ to $(1.12 \pm 0.14) \times 10^{-6}$ S/cm, respectively (Table 3). These conductivities are in the range of what has previously been achieved [35,42] and are adequate for the transfer of bioelectrical signals *in vivo* due to the low micro-current in the body [35,43]. It is clear that the conductivities of the hydrogels increased with an increase in AT content, and therefore, the conductivities could be adjusted by changing the amount of AT when formulating the hydrogels. Conventional high molecular weight conductive polymers have many practical problems in tissue engineering applications, such as poor polymer–cell interactions, the absence of cell interaction sites, hydrophobicity and poor solubility [25,44]. Coupling electrically conductive AT with hydrophilic, non-toxic, degradable and soluble hemicellulose is a promising solution to overcome the aforementioned drawbacks of previously utilized conductive polymers.

3.6. Swelling behavior of ECHHs

The swelling behavior is a key feature of hydrogels because their applications typically rely on their ability to absorb large amounts of water in a reproducible fashion. The swelling ratio (SR) of the hydrogels depends on the DS of C-AcGGM and the AT content (Fig. 7). Therefore, the SR could be tuned to meet the requirements of specific applications. The DS of MA proved to have a large effect on the swelling properties of the hydrogels (Fig. 7A). An increase in the amount of introduced MA to AcGGM led to a decrease in hydrogel swelling. The maximum SR of the hydrogels varied as follows: C1.0-AcGGM (DS = 1.14) < C0.5-AcGGM (DS = 0.60) < C0.25-AcGGM (DS = 0.24). This is due to a higher degree of cross-linking for the C1.0-AcGGM hydrogels compared to the C0.5-AcGGM (DS = 0.60) and C0.25-AcGGM (DS = 0.24) hydrogels. The crosslinking density calculated from swelling ratio is an important network parameter for composite hydrogels. The crosslinking density ($\overline{M}_c$) was calculated according to Peppas et al. [45], Eq. (4):

$$\frac{1}{\overline{M}_c} = \frac{2}{\overline{M}_n} - \frac{\left(\vartheta/V_1\right)\left[\ln\left(1-\vartheta_{2,s}\right)+\vartheta_{2,s}-\chi_1\vartheta_{2,s}\right]}{\vartheta_{2,s}^{1/3}-\frac{\vartheta_{2,s}}{2}} \tag{4}$$

here $\overline{M}_n$ is the number-average molecular weight of the polymer chain (substituted acetyl-galactoglucomannan); ϑ is the specific volume of the polymer, which is similar with that of dialdehyde konjac glucomannan [46], ~0.7 cm^3/g; V_1 is the molar volume of

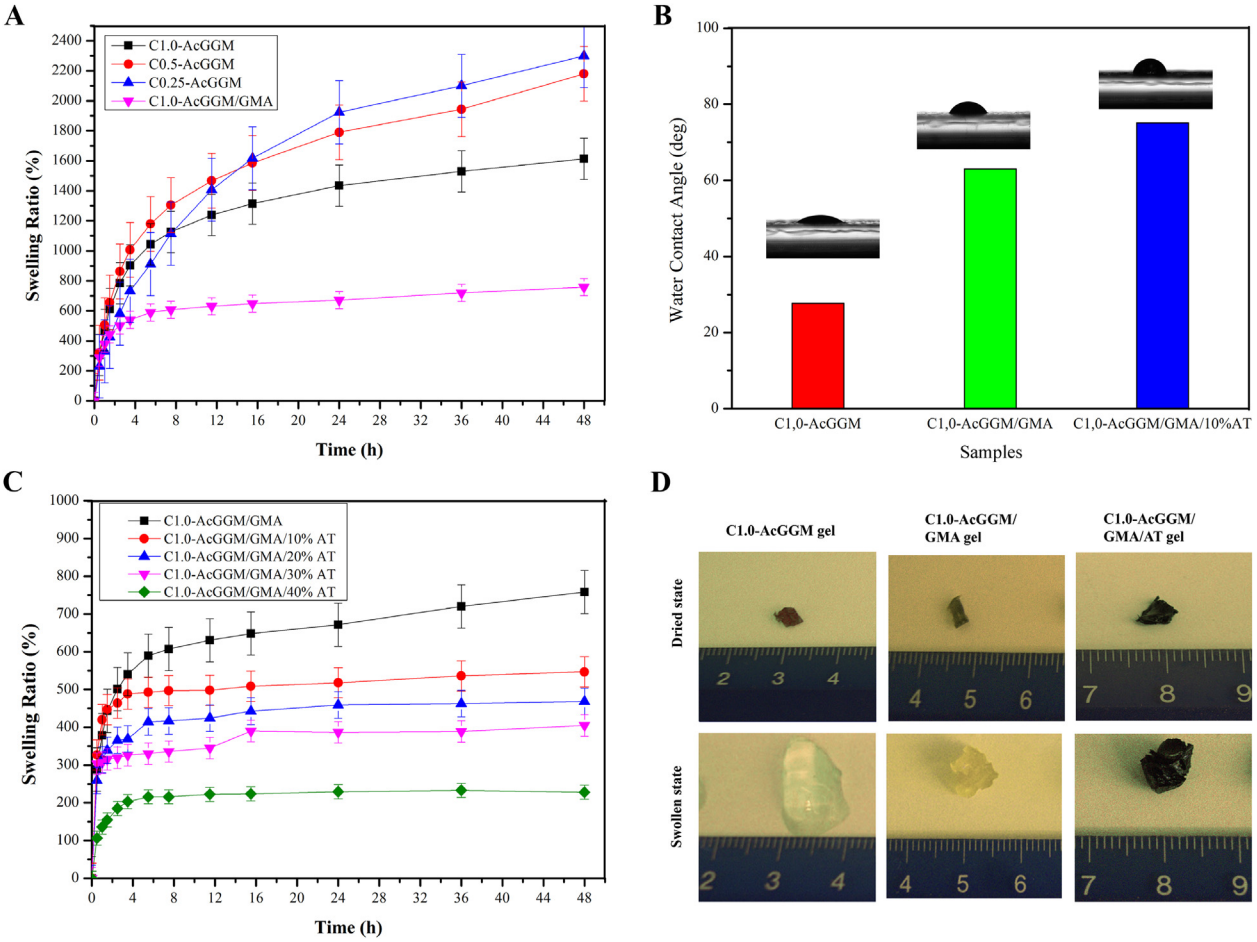

Fig. 7. Swelling ratios as a function of time of the different hydrogels (A and C); the water contact angle of C1.0-AcGGM, C1.0-AcGGM/GMA and C1.0-AcGGM/GMA/10%AT hydrogels films (B), and images of C1.0-AcGGM, C1.0-AcGGM/GMA and C1.0-AcGGM/GMA/10%AT hydrogels (D) in the dried and swollen state (48 h of swelling).

the swelling medium (18.06 cm^3/mol for water); the Flory–Huggins interaction parameter between polymer and water χ_1, which is similar with that of guar gum [47], $\chi_1 = 0.4940$; and the $\vartheta_{2,s}$ is relative with swelling ratio (SR^{-1}) [46]. The crosslinking densities ($\overline{M}_c$, g/mol) of C0.25-AcGGM, C0.5-AcGGM and C1.0-AcGGM hydrogels were 346, 335 and 273, respectively. The results demonstrated that the crosslinking density decreased with the increase of the DS of MA. The decrease in crosslinking density means less space for the accommodation of water in the network of these hydrogels, and decreases the flexibility of the uncrosslinked polymer chain, further leading to a decrease of the SR. The C0.5-AcGGM and C0.25-AcGGM hydrogels became softer after 48 h of swelling and did not retain their mechanical integrity as well as the C1.0-AcGGM hydrogels. Therefore, the latter were chosen for further investigations. A remarkable difference is seen when comparing C1.0-AcGGM/GMA with C1.0-AcGGM hydrogels. The SR of the former (758%) is less than half of the SR of the latter (1613%) after 48 h of swelling. Additionally, the swelling of C1.0-AcGGM/GMA hydrogels is much slower than that of C1.0-AcGGM hydrogels. To clarify the effect of the hydrophilicity of the hydrogels on SR, contact angles were measured [48]. The contact angles of C1.0-AcGGM and C1.0-AcGGM/GMA hydrogels films were 28° and 63° (Fig. 7B). It indicated that the introduction of GMA increased the hydrophobicity of the hydrogels, which makes difficult to adsorb water. After coupling with 10 wt. % of AT, the contact angle of the ECHH (C1.0-AcGGM/GMA/10%AT) increased up to 75° because of the hydrophobicity of AT, which resulted in a decrease in SR. The SR of the hydrogels containing covalently attached AT decreased with increasing AT content due to the hydrophobicity of AT. The C1.0-AcGGM/GMA hydrogel swelled most rapidly and had the highest SR (Fig. 7C). Compared to previous reports on other conductive hydrogels, the SR of ECHHs in the present study with the same weight percentage of AT are higher [31,39]. This is most likely due to the superior hydrophilicity of AcGGM compared with chitosan [31] and GMA-poly(ε-caprolactone)-PEG-poly(ε-caprolactone) [39]. Fig. 7D shows photographs of cut pieces of C1.0-AcGGM, C1.0-AcGGM/GMA and C1.0-AcGGM/GMA/10%AT hydrogels in dried and swollen states demonstrating the volume increase following 48 h of swelling.

3.7. Morphology of the hydrogels by scanning electron microscopy (SEM)

The morphological changes of the hydrogels before and after swelling also provide information on the swelling behavior of the hydrogels. SEM images of a cross-section of the C1.0-AcGGM (A), C1.0-AcGGM/GMA (B) and C1.0-AcGGM/GMA/20%AT (C) hydrogels in the dried state (A-1, B-1 and C-1) and the swollen state (48 h) after lyophilization (A-2, B-2 and C-2) are shown in Fig. 8. Before swelling, all hydrogels had a compact structure, while a homogenous macro-porous structure appeared after 48 h of swelling, indicating that these hydrogels swelled in a homogenous manner.

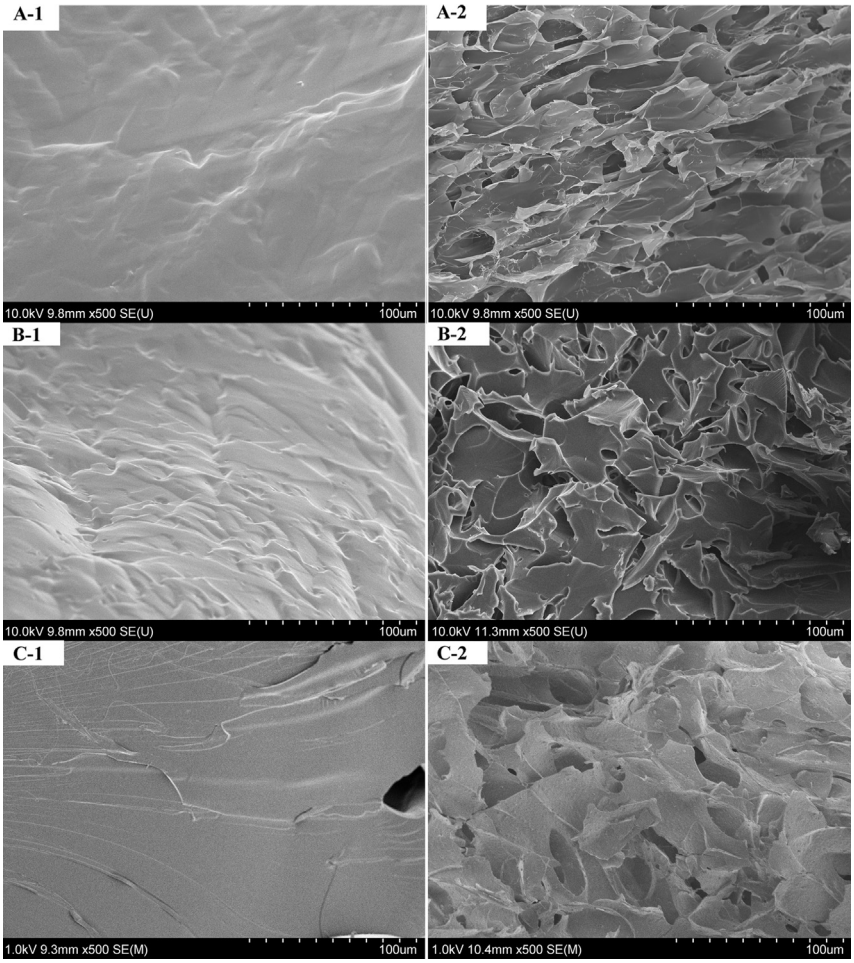

Fig. 8. SEM images of the cross-section of C1.0-AcGGM (A), C1.0-AcGGM/GMA (B) and C1.0-AcGGM/GMA/20%AT (C) hydrogels in the dry state (A-1, B-1 and C-1) and lyophilized from the swollen state at 48 h (A-2, B-2 and C-2). Magnification: ×500.

Interestingly, the C1.0-AcGGM hydrogels had larger pores with thinner walls, which could absorb a larger amount of water compared to the other hydrogels (C1.0-AcGGM/GMA and C1.0-AcGGM/GMA/20%AT). This confirms and explains the findings concerning the SR where the C1.0-AcGGM hydrogels had a high SR of 1613%, while the SR dropped to 758% for C1.0-AcGGM/GMA and to 468% for the C1.0-AcGGM/GMA/20%AT hydrogels. It becomes increasingly difficult for the water molecules to penetrate through the thicker walls in the hydrogels, and an increased hydrophobicity also decreases the SR. Therefore, the swelling rate of C1.0-AcGGM hydrogels is higher than those of C1.0-AcGGM/GMA and C1.0-AcGGM/GMA/20%AT hydrogels.

4. Conclusions

Electrically conductive hemicellulose hydrogels (ECHHs) have been successfully synthesized by a straight-forward and robust approach by introducing the conductive aniline tetramer (AT) into hydrophilic, non-toxic, and biocompatible hemicellulose networks. The ECHHs were prepared in two steps: first, carboxylated AcGGM (C-AcGGM) was dissolved with GMA followed by a polymerization initiated by ammonium persulfate; second, the formed hydrogels were covalently coupled with varying amounts of AT, which was homogeneously distributed throughout the network. C-AcGGM hydrogels were synthesized with 0.25, 0.5 and 1.0 eq of maleic anhydride and had swelling ratios (SR) of 2300%, 2180% and 1613%, respectively. By increasing of the AT content, the SRs were tuned from 548% to 228%, while simultaneously altering the conductivities by two orders of magnitude. The ability to control both swelling behavior and conductivity provides a wide range of material properties able to meet the needs of many specific applications.

Acknowledgments

The authors are grateful to the China Scholarship Council (CSC), ERC Advanced Grant, PARADIGM (Grant Agreement No. 246776) and The Royal Institute of Technology (KTH) for financial support for this work. Dr. Simon Leijonmarck at the Department of Applied Electrochemistry, School of Chemical Science in KTH is thanked for the kind support in the conductivity testing. Finally, our great appreciation goes to Professor Changsheng Zhao in Sichuan University for the generous help in applying to the scholarship from CSC.

Appendix A. Supplementary data

Supplementary data related to this article can be found at http://dx.doi.org/10.1016/j.polymer.2014.05.003.

References

[1] Appel EA, del Barrio J, Loh XJ, Scherman OA. Supramolecular polymeric hydrogels. Chem Soc Rev 2012;41(18):6195–214.
[2] Zhao WF, Fang BH, Li N, Nie SQ, Wei Q, Zhao CS. Fabrication of pH-responsive molecularly imprinted polyethersulfone particles for bisphenol-a uptake. J Appl Polym Sci 2009;113(2):916–21.
[3] Gao X, He C, Xiao C, Zhuang X, Chen X. Biodegradable pH-responsive polyacrylic acid derivative hydrogels with tunable swelling behavior for oral delivery of insulin. Polymer 2013;54(7):1786–93.
[4] Raic A, Rodling L, Kalbacher H, Lee-Thedieck C. Biomimetic macroporous PEG hydrogels as 3D scaffolds for the multiplication of human hematopoietic stem and progenitor cells. Biomaterials 2014;35(3):929–40.
[5] Lutolf MP. Spotlight on hydrogels. Nat Mater 2009;8(6):451–3.
[6] Patenaude M, Hoare T. Injectable, mixed natural-synthetic polymer hydrogels with modular properties. Biomacromolecules 2012;13(2):369–78.
[7] Paulino AT, Pereira AGB, Fajardo AR, Erickson K, Kipper MJ, Muniz EC, et al. Natural polymer-based magnetic hydrogels: potential vectors for remote-controlled drug release. Carbohydr Polym 2012;90(3):1216–25.
[8] Zhang X, Huang J, Chang PR, Li J, Chen Y, Wang D, et al. Structure and properties of polysaccharide nanocrystal-doped supramolecular hydrogels based on cyclodextrin inclusion. Polymer 2010;51(19):4398–407.
[9] Benavidez TE, Baruzzi AM. Comparative behavior of glucose oxidase and oxalate oxidase immobilized in mucin/chitosan hydrogels for biosensors applications. Polymer 2012;53(2):438–44.
[10] Zhao W, Jin X, Cong Y, Liu Y, Fu J. Degradable natural polymer hydrogels for articular cartilage tissue engineering. J Chem Technol Biotechnol 2013;88(3):327–39.
[11] Soderqvist Lindblad M, Albertsson AC, Ranucci E, Laus M, Giani E. Biodegradable polymers from renewable sources: rheological characterization of hemicellulose-based hydrogels. Biomacromolecules 2005;6(2):684–90.
[12] Lindblad MS, Ranucci E, Albertsson AC. Biodegradable polymers from renewable sources. New hemicellulose-based hydrogels. Macromol Rapid Commun 2001;22(12):962–7.
[13] Voepel J, Edlund U, Albertsson AC. Alkenyl-functionalized precursors for renewable hydrogels design. J Polym Sci Pol Chem 2009;47(14):3595–606.
[14] Edlund U, Albertsson AC. A microspheric system: hemicellulose-based hydrogels. J Bioact Compat Polym 2008;23(2):171–86.
[15] Peng XW, Ren JL, Zhong LX, Peng F, Sun RC. Xylan-rich hemicelluloses-graft-acrylic acid ionic hydrogels with rapid responses to pH, salt, and organic solvents. J Agric Food Chem 2011;59(15):8208–15.
[16] Bigand V, Pinel C, Perez DDS, Rataboul F, Huber P, Petit-Conil M. Cationisation of galactomannan and xylan hemicelluloses. Carbohydr Polym 2011;85(1):138–48.
[17] Ayoub A, Venditti RA, Pawlak JJ, Salam A, Hubbe MA. Novel hemicellulose-chitosan biosorbent for water desalination and heavy metal removal. ACS Sustain Chem Eng 2013;1(9):1102–9.
[18] Sun XF, Jing Z, Wang G. Preparation and swelling behaviors of porous hemicellulose-g-polyacrylamide hydrogels. J Appl Polym Sci 2013;128(3):1861–70.
[19] Roos AA, Edlund U, Sjoberg J, Albertsson AC, Stalbrand H. Protein release from galactoglucomannan hydrogels: influence of substitutions and enzymatic hydrolysis by beta-mannanase. Biomacromolecules 2008;9(8):2104–10.
[20] Gille S, Cheng K, Skinner ME, Liepman AH, Wilkerson CG, Pauly M. Deep sequencing of voodoo lily (Amorphophallus konjac): an approach to identify relevant genes involved in the synthesis of the hemicellulose glucomannan. Planta 2011;234(3):515–26.
[21] Maleki L, Edlund U, Albertsson AC. Unrefined wood hydrolysates are viable reactants for the reproducible synthesis of highly swellable hydrogels. Carbohydr Polym 2014;108:281–90.
[22] Green RA, Hassarati RT, Goding JA, Baek S, Lovell NH, Martens PJ, et al. Conductive hydrogels: mechanically robust hybrids for use as biomaterials. Macromol Biosci 2012;12(4):494–501.
[23] Guarino V, Alvarez-Perez MA, Borriello A, Napolitano T, Ambrosio L. Conductive PANi/PEGDA macroporous hydrogels for nerve regeneration. Adv Healthc Mater 2013;2(1):218–27.
[24] Heeger AJ. Semiconducting and metallic polymers: the fourth generation of polymeric materials (Nobel lecture). Angew Chem Int Ed 2001;40(14):2591–611.
[25] Guo BL, Glavas L, Albertsson AC. Biodegradable and electrically conducting polymers for biomedical applications. Prog Polym Sci 2013;38(9):1263–86.
[26] Guo BL, Sun Y, Finne-Wistrand A, Mustafa K, Albertsson AC. Electroactive porous tubular scaffolds with degradability and non-cytotoxicity for neural tissue regeneration. Acta Biomater 2012;8(1):144–53.
[27] Wang LX, SoczkaGuth T, Havinga E, Mullen K. Poly(phenylenesulfidephenylenamine) (PPSA) – the ('compound') of polyphenylenesulfide with polyaniline. Angew Chem Int Ed 1996;35(13–14):1495–7.
[28] Liu YD, Hu J, Zhuang XL, Zhang PB, Wei Y, Wang XH, et al. Synthesis and characterization of novel biodegradable and electroactive hydrogel based on aniline oligomer and gelatin. Macromol Biosci 2012;12(2):241–50.
[29] Hu J, Huang LH, Zhuang XL, Zhang PB, Lang L, Chen XS, et al. Electroactive aniline pentamer cross-linking chitosan for stimulation growth of electrically sensitive cells. Biomacromolecules 2008;9(10):2637–44.
[30] Jacobs A, Dahlman O. Characterization of the molar masses of hemicelluloses from wood and pulps employing size exclusion chromatography and matrix-assisted laser desorption ionization time-of-flight mass spectrometry. Biomacromolecules 2001;2(3):894–905.
[31] Guo BL, Finne-Wistrand A, Albertsson AC. Facile synthesis of degradable and electrically conductive polysaccharide hydrogels. Biomacromolecules 2011;12(7):2601–9.
[32] Voepel J, Sjoberg J, Reif M, Albertsson AC, Hultin UK, Gasslander U. Drug diffusion in neutral and ionic hydrogels assembled from acetylated galactoglucomannan. J Appl Polym Sci 2009;112(4):2401–12.
[33] Saadatmand S, Edlund U, Albertsson AC, Danielsson S, Dahlman O, Karlstrom K. Turning hardwood dissolving pulp polysaccharide residual material into barrier packaging. Biomacromolecules 2013;14(8):2929–36.
[34] Marcasuzaa P, Reynaud S, Ehrenfeld F, Khoukh A, Desbrieres J. Chitosan-graft-Polyaniline-based hydrogels: elaboration and properties. Biomacromolecules 2010;11(6):1684–91.
[35] Guo BL, Finne-Wistrand A, Albertsson AC. Degradable and electroactive hydrogels with tunable electrical conductivity and swelling behavior. Chem Mater 2011;23(5):1254–62.

[36] Parsa A, Ab Ghani S. The improvement of free-radical scavenging capacity of the phosphate medium electrosynthesized polyaniline. Electrochim Acta 2009;54(10):2856–60.
[37] Chen R, Benicewicz BC. Preparation and properties of poly(methacrylamide)s containing oligoaniline side chains. Macromolecules 2003;36(17):6333–9.
[38] Huang LH, Hu J, Lang L, Wang X, Zhang PB, Jing XB, et al. Synthesis and characterization of electroactive and biodegradable ABA block copolymer of polylactide and aniline pentamer. Biomaterials 2007;28(10):1741–51.
[39] Guo BL, Finne-Wistrand A, Albertsson AC. Versatile functionalization of polyester hydrogels with electroactive aniline oligomers. J Polym Sci Pol Chem 2011;49(9):2097–105.
[40] Liu Y, Cui H, Zhuang X, Zhang P, Cui Y, Wang X, et al. Nano-hydroxyapatite surfaces grafted with electroactive aniline tetramers for bone-tissue engineering. Macromol Biosci 2013;13(3):356–65.
[41] Guo BL, Finne-Wistrand A, Albertsson AC. Universal two-step approach to degradable and electroactive block copolymers and networks from combined ring-opening polymerization and post-functionalization via oxidative coupling reactions. Macromolecules 2011;44(13):5227–36.
[42] Chao D, Ma X, Liu Q, Lu X, Chen J, Wang L, et al. Synthesis and characterization of electroactive copolymer with phenyl-capped aniline tetramer in the main chain by oxidative coupling polymerization. Eur Polym J 2006;42(11):3078–84.
[43] Niple JC, Daigle JP, Zaffanella LE, Sullivan T, Kavet R. A portable meter for measuring low frequency currents in the human body. Bioelectromagnetics 2004;25(5):369–73.
[44] Guimard NK, Gomez N, Schmidt CE. Conducting polymers in biomedical engineering. Prog Polym Sci 2007;32(8–9):876–921.
[45] Peppas NA, Hilt JZ, Khademhosseini A, Langer R. Hydrogels in biology and medicine: from molecular principles to bionanotechnology. Adv Mater 2006;18(11):1345–60.
[46] Yu H, Lu J, Xiao X. Preparation and properties of novel hydrogels from oxidized konjac glucomannan cross-linked chitosan for in vitro drug delivery. Macromol Biosci 2007;7(9–10):1100–11.
[47] Li XY, Wu WH, Wang JQ, Duan YF. The swelling behavior and network parameters of guar gum/poly(acrylic acid) semi-interpenetrating polymer network hydrogels. Carbohydr Polym 2006;66(4):473–9.
[48] Zhao WF, Huang JY, Fang BH, Nie SQ, Yi N, Su BH, et al. Modification of polyethersulfone membrane by blending semi-interpenetrating network polymeric nanoparticles. J Membr Sci 2011;369(1–2):258–66.